Pakistan Veterinary Journal

ISSN: 0253-8318 (PRINT), 2074-7764 (ONLINE)
DOI: 10.29261/pakvetj/2026.019

RESEARCH ARTICLE

Demographics and Conservation Hotspots of PPR-Susceptible Ungulates in Huaitoutala, Qinghai, China

HaoNing Wang [1,2], Xin Fan [3,4], GuanYing Ni [5], FuYun Chen [5], RenNa Wu [5], ShiFeng Sui [6], XiaoDi Wang [1,2], ShaoPeng Yu [1,2,*], XiaoDong Wu [7,*] and XiaoLong Wang [3,4,*]

[1]Heilongjiang Cold Region Wetland Ecology and Environment Research Key Laboratory, School of Geography and Tourism, Harbin University, 109 Zhongxing Road, Harbin 150086, Heilongjiang Province, P. R. China; [2]School of Geography and Tourism, Harbin University, Harbin 150086, Heilongjiang Province, P. R. China; [3]College of Wildlife and Protected Area, Northeast Forestry University, Harbin 150040, Heilongjiang province, P. R. China; [4]Key Laboratory for Wildlife Diseases and Bio-Security Management of Heilongjiang Province, Harbin 150040, Heilongjiang Province, P. R. China; [5]Haixi Animal Disease Control Center, Delingha 817099, Qinghai Province, P. R. China; [6]Zhaoyuan Forest Resources Monitoring and Protection Service Center, Zhaoyuan 265400, Shandong province, P. R. China; [7]China Animal Health and Epidemiology Center, Qingdao 266032, Shandong Province, P. R. China
*Corresponding author: ecorisk88@163.com

ARTICLE HISTORY (26-033)

Received: January 08, 2026
Revised: February 11, 2026
Accepted: February 13, 2026
Published online: February 26, 2026

Key words:
Peste des Petits Ruminants (PPR)
Population Density
PPR virus (PPRV)
Species Distribution Modeling
Wildlife Reservoirs
Zoonotic Interfaces

ABSTRACT

Peste des petits ruminants (PPR) is a viral illness that is highly transmissible and poses a great threat to livestock production, as well as biodiversity protection at an international level. Despite the current vaccination drives, the spread of the PPR virus (PPRV) host range into wildlife populations is undermining eradication efforts, with documented cases of cross-species transmission intensifying control challenges. This study combines field investigation and ecological simulations in a systematic assessment of the threat of PPRV spillover to vulnerable wildlife species within Huaitoutala in China in Qinghai Province. The four vulnerable species were determined in the study: goitered gazelle (*Gazella subgutturosa*), bharal (*Pseudois nayaur*), argali (*Ovis ammon*) and wild yak (*Bos mutus*). The field transects (315 km) showed population of gazelles, bharal, argali and wild yaks per unit area as 0.329, 0.302, 0.193 and 0.100, respectively. The most key ecological drivers were discovered as being diurnal temperature range, which was the most significant to influence gazelle distribution and anthropogenic factors, such as human settlement density, which played a significant role in habitat choice by bharal and argali with the help of MaxEnt modeling. This study presents an initial ecological risk assessment, identifying areas where wildlife-livestock interfaces may facilitate potential PPRV spillover. While the approach offers a framework for prioritizing surveillance zones in data-deficient highland systems, it does not confirm active viral transmission. These findings provide ecological guidance to support future targeted serological and virological investigations and strengthen the wildlife component of the Global Eradication Programme. The novel ecological methodology establishes a new concept framework for combating transboundary animal diseases through multi-scale risk prediction.

To Cite This Article: Wang HN, Fan X, Ni GY, Chen FY, Wu RN, Sui SF, Wang XD, Yu SP, Wu XD and Wang XL, 2026. Demographics and conservation hotspots of ppr-susceptible ungulates in huaitoutala, qinghai, china. Pak Vet J. http://dx.doi.org/10.29261/pakvetj/2026.019

INTRODUCTION

Peste des petits ruminants (PPR) is an acute and very contagious illness resulting in the causation of the PPR virus (PPRV), which is found in small ruminants like goats and sheep. PPRV is a family of Paramyxoviridae and is an antigen and genetically connected with the measles and Newcastle disease causing viruses. After a 4-6 days incubation most of the infected animals typically fall ill with signs of fever, death of mouth tissue, diarrhea and pneumonia with a high mortality rate and considerable economic consequences on the small ruminant industry (Jones *et al.*, 2016). PPRV was first documented in Africa in the 1940s (Dou *et al*., 2020). Since then, its geographic range

has expanded steadily and the disease is now reported in roughly 75 countries across Africa, Asia, the Middle East and parts of Europe (Baazizi *et al*., 2017). Evidence of continued circulation was provided by an outbreak recorded in Rwanda in October 2023, suggesting that transmission has not only persisted but has also reached additional areas (Lembo *et al*., 2013). Estimates from the last twenty years indicate that PPR has affected no fewer than 30 million animals worldwide, reflecting the long-term and widespread nature of the disease burden (Benfield *et al*., 2021).

In addition to the devastating impact on livestock, habitat fragmentation and the migration of wild ungulate populations caused by human activities and climate change are altering the interactions between global wildlife and livestock. These changes may increase the risk of PPRV interspecies transmission. An increasing number of studies have documented the involvement of wildlife in the epidemiology of PPRV. Several wild ruminant species, including gazelles and antelopes, are known to be susceptible to infection. Contact at shared grazing grounds and water points provides opportunities for virus transmission within natural systems (Munir *et al*., 2014). Evidence from Pakistan further illustrates this process, where serological surveys in sheep and wild goats (*Capra aegagrus*) have revealed natural spillover events, suggesting ongoing but largely unrecognized circulation between mountain ungulates and domestic livestock in areas of habitat overlap (Aziz *et al*., 2016).

In 2015, the Global PPR Eradication Programme (PPR-GEP) was started because PPRV can infect a wide range of species, with the goal of eradicating the disease by 2030 through planned vaccination and surveillance. However, rising incidence of PPRV infections in wildlife poses a challenge to traditional vaccination strategies for livestock (Bouchemla *et al*., 2020). Sowjanya *et al*. (2021) systematically reviewed PPRV prevalence and found high seroprevalence rates in African species, indicating broad exposure. Similarly, studies in Pakistan have identified the interface between domestic goats and the Sindh ibex as a major risk for virus transmission (Wensman *et al*., 2018). The presence of PPRV infection in free-ranging wild ungulates has been reported in multiple areas, the outbreak in the critically endangered Mongolian saiga antelope (*Saiga tatarica mongolica*) is a case that demonstrated the vulnerability of wild populations (Benfield *et al*., 2021). The sero-epidemiological surveys in Asia and Africa further highlight the role of wildlife as a potential reservoir for PPRV (Sowjanya *et al*., 2021). The seroprevalence survey in Asia and Africa also highlights the contribution of wildlife to the possible reservoirs of PPRV (Sowjanya *et al.*, 2021).

One of the main concerns of Global Eradication Programme (GEP) is the scarcity of research on high altitude ecosystems where there is a high amount of coexistence of wildlife and livestock. Zahur *et al.* (2011) also report that the seroprevalence rate among wild goats (*Capra aegagrus*) in the northern mountains of Pakistan was 35% and that an adjacent farm goat had only 12% rate, highlighting the inefficiency of vaccination approaches that can be applied to domestic animals (Zahur *et al*., 2011). More importance is becoming more apparent in ecological models in the control of PPR. A spatial transmission model that pointed at 14 counties that are in high risk due to their closeness to the international borders; yet there is no available wildlife population density data, which is a barrier to effective prediction (Gao *et a*l., 2021). According to Liu *et al*. 63 percent of new epidemics in 2007-2017 were located within 50 km of the nature reserves buffer zones (Liu *et al.*, 2018), which as terrain fragmentation is more dependent on contact between animals (Harman *et al*., 2024). However, existing surveillance mechanisms only pay attention to farms, which means that the dynamic wildlife data is extremely insufficient. An example is that the population estimates of wild yaks (*Bos mutus*) in Haixi Prefecture, Qinghai Provinces still rely on aerial surveys done in 2008 (Harris *et al.*, 2010); which probably puts a strong underestimation on transmission risks in these ecologically sensitive areas.

This study aims to bridge such research gaps by developing an interdisciplinary model on the assessment of PPR risk. We integrate field transect-acquired data on population and a climate-sensitive ecosystem model to predict high-risk interface areas. The key relevant innovation is that transect-based field data have been mixed with ecological modeling on a first-time basis that is likely to present an effective long-sighted monitoring system in areas of low vaccine coverage and the future provision of the goal of 2030 on the GEP.

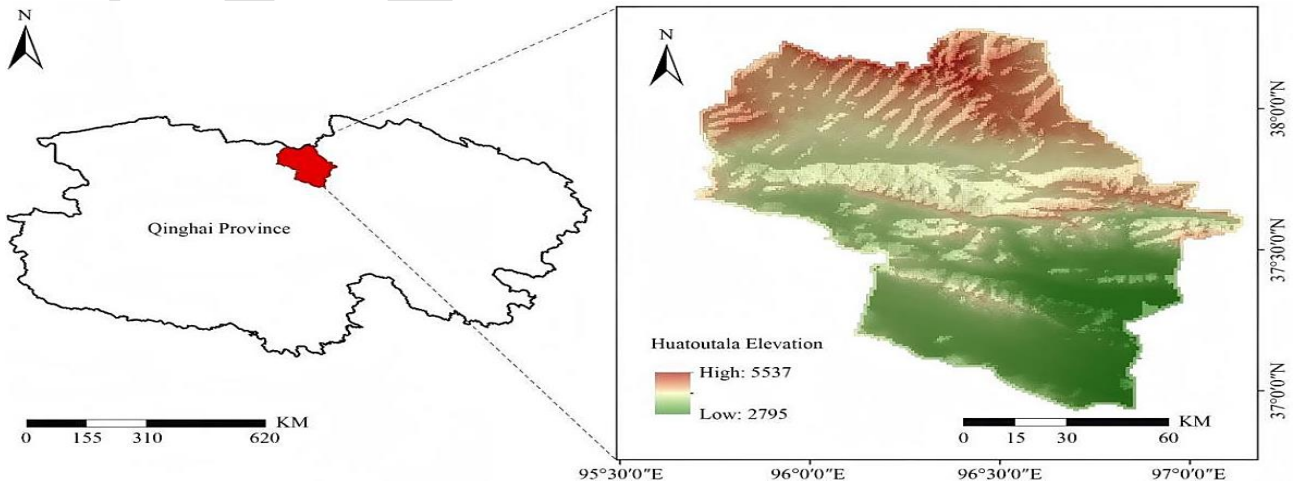

Fig. 1: Study area of Huaitoutala, Qinghai Province, China (Data source : The map showing the administrative boundaries of Huaitoutala in Qinghai Province was sourced from the Resource and Environment Science Data Center at the Chinese Academy of Sciences (https://www.resdc.cn/.)

MATERIALS AND METHODS

Study area: Huaitoutala Town is in Qinghai Province in the northeast part of Qaidamu Basin, China. It is located in the northwestern part of Haixi Mongolian and Tibetan Autonomous Prefecture, and west of Delingha City (Fig. 1). The town is situated along the Kelu lake shore, and the topography of the area is steep (north to south) with mountains and hills occupying about four-fifths of the area. The region has a continental plateau climate and is mainly arid with an average temperature of 2.4°C per annual and an average yearly rainfall of 90.1 mm. The Balenggeng River is the principal river in the region, that is started off the Zongwulong Mountain and flows as an internal river.

Huaituotala has unique ecological and climatic condition provide crucial habitat for a variety of wildlife species, supporting over a dozen animals including the bharal (*Pseudois nayaur*), goitered gazelle (*Gazella subgutturosa*) and snow leopard *(Panthera uncia*). The most common of these include the wild yak (*Bos mutus*), Tibetan wild ass (*Equus kiang*), and the snow leopard *(Panthera uncia*) that are first-level national protected animals. Other species, such as the argali (*Ovis ammon*), bharal (*Pseudois nayaur*), goitered gazelle (*Gazella subgutturosa*), brown bear (*Ursus arctos*), lynx (*Lynx lynx*) and whooper swan (*Cygnus cygnus*) are designated as second-level national protected animals. This highlights the region's significant biodiversity and ecological importance.

Field transect survey: Wildlife distribution data were primarily obtained from the Forestry and Grassland Bureau of Haixi Mongolian and Tibetan Autonomous Prefecture, the Delingha Animal Epidemic Prevention and Control Center, the Yikla Nature Reserve Station, and the Yashatu Nature Reserve Station. The other data was gathered by searching the Qinghai animal chronicles, interviewing the local nomadic people, and conducting the field search. These approaches helped identify areas with high potential for wildlife presence.

Five survey transects were established at the following locations: snow pasture (5500m), Kekexili Mountain and the Tataleng River (3500m), Zongwulong Mountain (5000m), Buyitan Ula Mountain (4000m) and Crooked Lake (2700m) (Fig. 2). The transects were distributed evenly from south to north to minimize sampling bias and covered all habitat types from Crooked Lake to the snow pasture, with intervals exceeding 10km. Each transect ranged from 30 to 62km in length, totaling 315km.

Researchers traversed each transect at speeds of 30-45 km h^{-1}, estimating sizes of wildlife groups (recorded as group units), and documenting species, sampling time, location, weather, and other environmental factors. GPS devices and distance-measuring tools from the GPS toolbox were used to record encountered animals, along with the vertical distance to the animals and the geographic coordinates of the observer.

Population density calculation: The population density of each species was estimated using the Distance package in R 4.3.2 with the following formula (Equation (1-1)):

$$\hat{D} = \frac{n\hat{f}(0)\hat{E}}{2L} \quad (1\text{-}1)$$

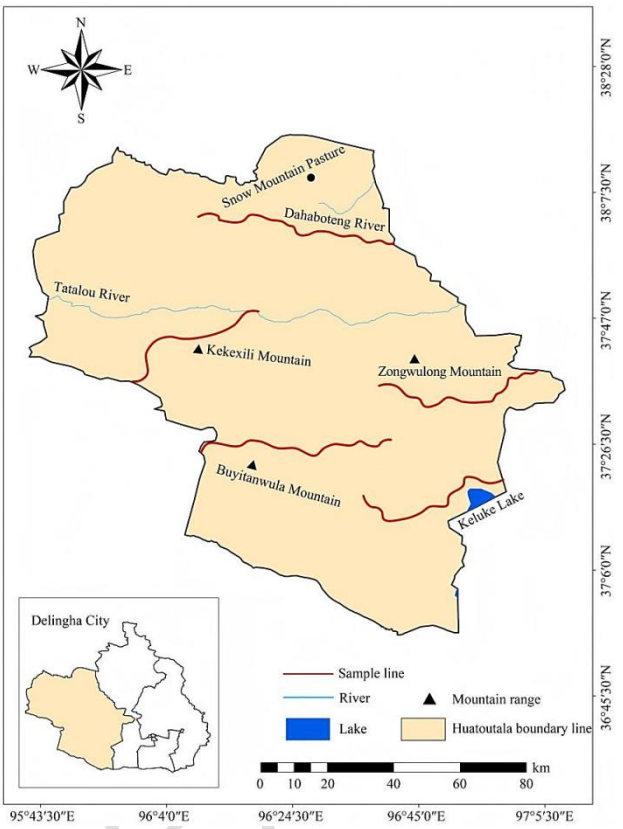

Fig. 2: Survey transect layout for assessing ungulate population density. The diagram illustrates the distribution of five transect lines across different elevations and habitat types within the study area, covering snow-capped pastures, rivers, and mountain ranges.

where $\hat{D}$ is the number of individuals per square kilometer; n is the number of observed groups of the target species; $\hat{f}(0)$ denotes the estimated probability density function of detection at zero vertical distance; $\hat{E}$ represents the expected group size of the target species; and L is the total length of all transects (in kilometers) (Thomas *et al*., 2010).

In Equation (1-1), the value of $\hat{f}(0)$ depends on $g(x)$, which indicates the likelihood of spotting an animal at a vertical distance of zero. It is presumed that animals located at zero distance are all detected, meaning $g(x) = 1$. The population density $\hat{D}$ can thus be estimated via the detection function, as expressed in Equation (1-2):

$$f(0) = \frac{1}{\int_0^w g(x)dx} \quad (1\text{-}2)$$

where w represents the transect width, and x denotes the vertical distance from the transect line. The detection function $g(x)$ was modeled using three key forms: half-normal, uniform, and hazard-rate. For these corrections, cosine, Hermite polynomial, and basic polynomial series expansions were applied as needed. All statistical procedures were carried out in RStudio with the Distance

package. Detection functions were fitted using the ds function, with the truncation distance fixed at 1km to improve the stability of the estimates. To limit the influence of extreme observations and potential measurement error, a 5% right truncation was applied. The detection function was specified by selecting the appropriate 'key' option. Where adjustment terms were added using the 'adjustment' setting to improve the fit of the model. Models were compared using the Akaike Information Criterion, and selection was based on the lowest AIC value. Results from the chosen model were obtained with the summary function and used for further analysis.

Prediction of suitable distribution for PPRV-susceptible wildlife

Data collection: Occurrence data of oitered gazelle, bharal, argali and wild yak were then gathered from several sources included published studies from CNKI, the Global Biodiversity Information Facility (https://www.gbif.org/), reports available from social media, and observations collected during fieldwork. After screening, 389 records were retained for further analysis, including 143 for goitered gazelle, 162 for bharal, 44 for argali, and 40 for wild yak.

Table 1: Research environmental variables

Category	Description	Unit	Data Abbreviation
Environmental Variables	The mean temperature of months 1–12	°C	temp1-temp12
	Maximum temperature of months 1–12	°C	tmax1-tmax12
	Minimum temperature of months 1–12	°C	tmin1-tmin12
	Precipitation of months 1–12	mm/mouth	prec1-prec12
Bioclimatic Factors	Annual mean temperature	°C	bio1
	Mean monthly diurnal range (Tmax-Tmin)	°C	bio2
	Isothermality (bio2/bio7) × 100	Ratio	bio3
	Temperature seasonality (Standard deviation)	°C	bio4
	Maximum temperature of the warmest month	°C	bio5
	Minimum temperature of the coldest month	°C	bio6
	Annual temperature range (bio5-bio6)	°C	bio7
	The mean temperature of the wettest quarter	°C	bio8
	The mean temperature of the driest quarter	°C	bio9
	The mean temperature of the warmest quarter	°C	bio10
	The mean temperature of the coldest quarter	°C	bio11
	Annual precipitation	Mm	bio12
	Precipitation of the wettest month	Mm	bio13
	Precipitation of the driest month	Mm	bio14
	Precipitation seasonality (Coefficient of variation)	Fraction	bio15
	Precipitation of the wettest quarter	Mm	bio16
	Precipitation of the driest quarter	Mm	bio17
	Precipitation of the warmest quarter	Mm	bio18
	Precipitation of the coldest quarter	Mm	bio19
Elevation	Elevation	m a.s.l.	dem
Population density	Human population density	People/km^2	popu
Land use	Cropland (10), rice paddy (11), forest (20), Grassland (30), shrubland (40), permanent snow and ice (100), cloud (120), Grassland (130), sparse vegetation (fc < 0.15) (150), wetlands (180), impervious (190), bare area (200), unconsolidated bare area (202), water body (210), permanent ice and snow (220).		land

Environmental variables included both biotic/abiotic factors and anthropogenic influences such as human population density, elevation, and land use types (Table 1). Sixty-seven climatic variables were retrieved from the WorldClim database (http://www.worldclim.org/) with a resolution of 30 arcseconds, approximately 1km. WorldPop (http://www.worldpop.org.uk/data/) provided the population density data, and SoilGrids supplied the land use data. (http://www.isric.org/explore/soilgrids). All spatial layers were processed and clipped to the study area boundaries using ArcGIS 10.9. Data were aligned to the UTM-WGS-1984 coordinate system and adjusted to a uniform 30 arc-second resolution.

Data preprocessing: The SDM Toolbox v2.5c in ArcGIS 10.8 was used to decrease the spatial autocorrelation of species occurrence points (Brown *et al*., 2017). Distances ranging from 0 to 10 km were filtered and tested, the MaxEnt model was employed to assess suitable distribution areas for each species at every distance threshold. Environmental data for the four species across 67 variables were extracted in ArcGIS 10.8 to construct an environmental data matrix. To reduce redundancy among environmental predictors and avoid model overfitting, a multistep variable selection procedure was applied prior to species distribution modeling. Initially, Principal Component Analysis (PCA) was conducted on the extracted environmental variables to identify dominant gradients in the data (Moriguchi *et al*., 2016). Only principal components with eigenvalues greater than 1 were retained, ensuring that variables included in subsequent analyses contributed meaningful explanatory power. Environmental variables with loadings exceeding 0.95 within these components were chosen as candidate predictors (Fekede *et al*., 2019). To further control for multicollinearity, variance inflation factor (VIF) analysis was performed and the value should not exceed 10 indicating acceptable multicollinearity (Duque-Lazo *et al*., 2016). Variables with VIF≥10 were iteratively removed until all remaining predictors met the acceptable collinearity threshold. (Pittiglio *et al*., 2012). Higher collinear variables identified in the MaxEnt model were excluded based on their lower contributions (Van Gils *et al*., 2014). Final environmental variables were selected based on a combination of statistical contribution and ecological relevance, ensuring that predictors retained in the model reflected both numerical robustness and known ecological drivers of ungulate distribution in high-altitude environments.

Model prediction: Species distribution modeling was conducted using the Maximum Entropy (MaxEnt) algorithm, which is well suited for presence-only data and has been widely applied in wildlife distribution studies with limited occurrence records. To evaluate model performance and reduce sampling bias, occurrence data of the species were randomly partitioned with 70 percent for model training and 30 percent reserved for testing where the data is in a logistic output format. Model robustness was enhanced by running ten bootstrap replicates, allowing estimation uncertainty to be incorporated into the final predictions. All other model parameters were kept at default settings to avoid unnecessary model complexity. Prior to modeling, spatial autocorrelation among

occurrence points was reduced using SDM Toolbox (v2.5c) in ArcGIS, ensuring that clustered records did not disproportionately influence model outcomes. To assess the performance of the model, the Receiver Operating Characteristic (ROC) curve was employed which plots the true positive rate (sensitivity) against the false positive rate (1-specificity) (Pepe *et al.,* 2009). Assessment of predictive accuracy used the area under the curve (AUC), where higher values indicate better performance and a stronger correlation between environmental variables and model predictions. The definition of the AUC was as follows, 0.5-0.6 was poor, 0.6-0.7 was moderate, 0.7-0.8 was reliable, 0.8-0.9 was good and 0.9-1.0 was excellent. It was considered a high standard deviation (SD) to exclude cases of erroneous variables and refine the ROC curve (Duque-Lazo *et al.,* 2018).

RESULTS

Population density of four PPRV-susceptible wildlife species in Huatoutala: The hazard rate and half-normal together with uniform distribution gave rise to different models of the detection function. The model with the lowest AIC value was selected as the optimal model (Tables 2 and Table 3). The detection functions of each species were overlaid together with vertical distance histograms (Fig. 3). In the case of goitered gazelle (Fig. 3a), the detectability of the animal dropped drastically as range increased, which means that it was more detectable at the lower ranges. The trend can be interpreted as preference of the species to open landscape and visibility where it is easily detected when conducting transect surveys. On the contrary, the curve of detection of bharal (Fig. 3b) decreased more slowly, indicating that they have a wider range of detection presumably because of their propensity to develop large groups and inhabit rocky slopes, in which movement and group size increases the visibility notwithstanding the rugged topography. In the case of argali (Fig. 3c), the detection function declined sharply for short distances, with most sightings occurring nearby. This pattern may be related to limited visibility in steep and rocky habitats, where observation conditions are often poor, and could also indicate that groups are more scattered or loosely organized. In comparison, the detection curve for wild yak (Fig. 3d) was relatively flat, with only a slight increase observed at intermediate distances. Detection probability remained low across most distance intervals.

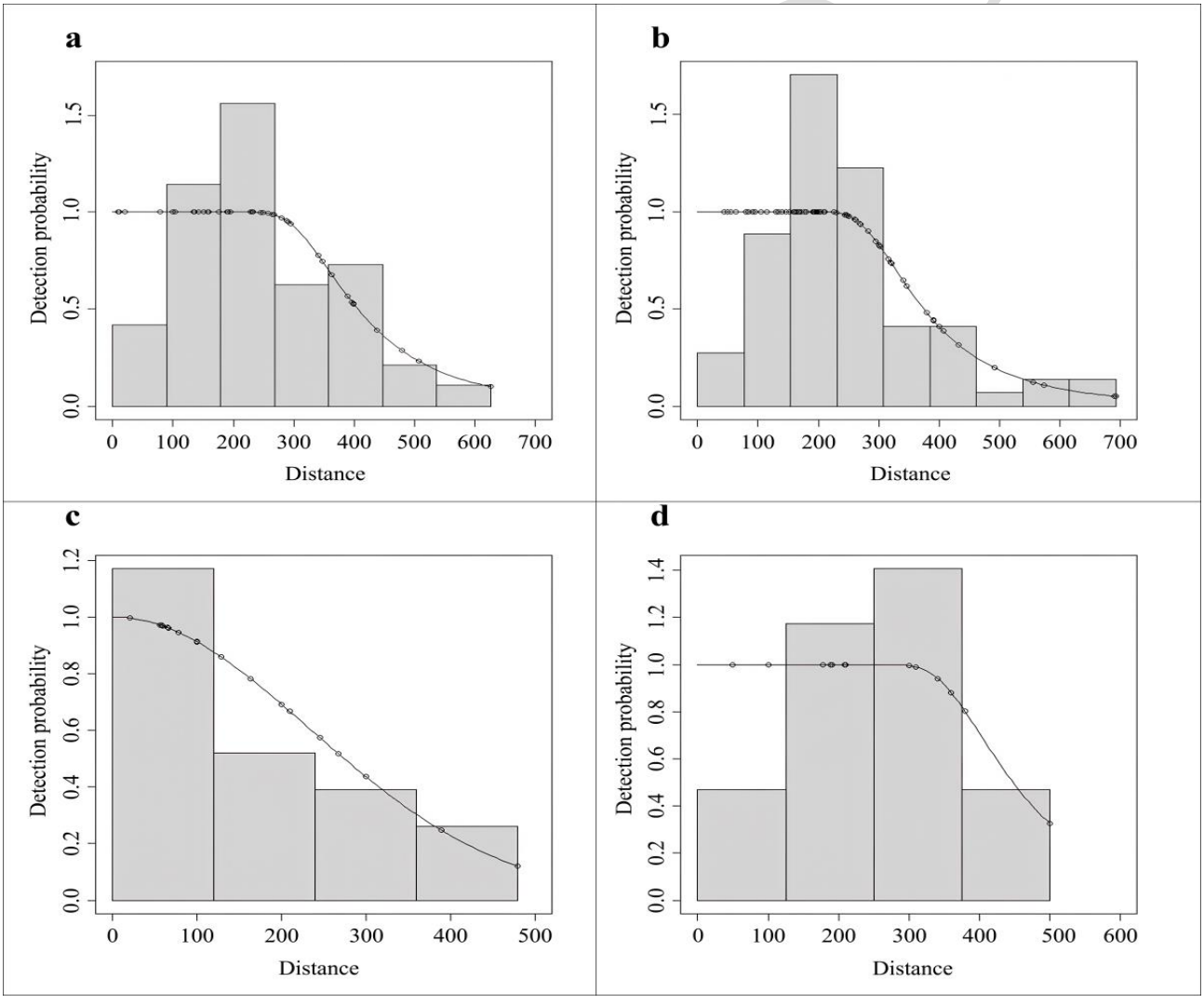

Fig. 3: Detection probability histograms versus vertical distance for four PPRV-susceptible wildlife species. Panels show the vertical distance histograms and fitted detection probability curves for: (a) *Goitered gazelle* (*Gazella subgutturosa*); (b) Bharal (*Pseudois nayaur*); (c) Argali (*Ovis ammon*); and (d) Wild yak (*Bos mutus*). These plots were generated using distance sampling analysis for density estimation

Table 2: Akaike information criterion for different combinations of models

Model	Goitered Gazelle	Bharal	Argali	Wild Yak
Half-normal	583.8267	978.4231	219.1656	188.4282
Half-normal + Cosine	583.6345	976.2408	219.1656	188.4282
Half-normal + Hermite polynomial	583.4985	977.1350	219.1656	188.4282
Half-normal + Simle polynomial	583.8267	978.4231	219.1656	188.4282
Hazard-rate	581.9087	971.7764	220.0130	189.6853
Hazard-rate + Cosine	581.9087	971.7764	220.0130	189.6853
Hazard-rate + Hermite polynomial	581.9087	971.7764	220.0130	189.6853
Hazard-rate + Simle polynomial	581.9087	971.7764	220.0130	189.6853
Uniform	592.4746	1007.2787	222.1786	186.4382
Uniform + Cosine	582.5829	976.509	218.6048	186.4382
Uniform + Hermite polynomial	585.5469	979.6591	221.6318	186.4382
Uniform + Simle polynomial	583.9009	978.1444	220.6178	186.4382

Table 3: Population density assessment parameters for four species

Indicator	Goitered Gazelle	Bharal	Argali	Wild Yak
Optimal model (key + adjustment)	Hazard-rate + Cosine	Hazard-rate + Cosine	Half-normal + Cosine	Uniform + Cosine
Density(ind./km^2)	0.329	0.302	0.193	0.100
95% confidence interval for density	0.155~0.699	0.074~1.239	0.068~0.549	0.034~0.289
Distant range(m)	626	693	479	500

During the surveys, 228 goitered gazelles were recorded. These observations comprised 46 separate groups. Group size was variable and ranged from one individual to a maximum of 30. The estimated population density was 0.329 individuals km^{-2}. The corresponding 95% confidence interval ranged from 0.155 to 0.699; Surveys of bharal recorded 982 individuals. These were distributed among 77 groups. Group size ranged between 3 and 100 individuals. Population density was estimated at 0.302 individuals km^{-2}, with a 95% confidence interval of 0.074-1.239; Argali populations were less abundant, with 100 individuals in 18 groups (1-20 individuals) and a density of 0.193 individuals km^{-2} (95%CI: 0.068–0.549). Wild yaks were the least numerous, with 132 individuals recorded in 15 groups (1-50 individuals). An estimated density of 0.100 individuals per km^2 was determined (95% confidence interval: 0.034-0.289). The effective strip widths were 626 meters for goitered gazelle, 693 meters for bharal, 479 meters for argali, and 500 meters for wild yak (Table 3).

Spatial autocorrelation filtering: To reduce spatial autocorrelation, we applied spatial filtering to the distribution points of PPRV-susceptible wildlife using SDM Toolbox v2.5c in ArcGIS 10.8. Minimum distance thresholds from 0 to 10 km (in 1-km intervals) were tested. The optimal thresholds—yielding the highest AUC values and most stable models—were 1 km for goitered gazelle, bharal, and wild yak, and 0 km for argali. At these distances, the following numbers of distribution points were retained for subsequent modeling: goitered gazelle (92), bharal (66), argali (43), and wild yak (35).

Dimensionality reduction of environmental variables: PCA was performed on environmental variables extracted from species distribution points (Table 4). For the goitered gazelle, four principal components (eigenvalues>1) collectively explained 96.456% of the variance. Similarly, four components were retained for the bharal, accounting for 95.508% of the cumulative variance. In the case of argali, three factors accounted 96.164% of the variance and three factors also accounted for 97.165% in case of wild yak. After VIF analysis and refinement of the MaxEnt model, important environmental predictors were found when applied to each species (Table 5). In the case of goitered gazelle, dem (50.4%), bio2 (28.6%), bio7 (10.8%) and pop (10.2) were the variables that significantly contributed to the results with VIF 1.02 to 6.25 (Table 5 and Fig. 4a). In the case of bharal, the variables that were chosen consisted of popu (47.9%), prec10 (16.7%), bio7 (12.7%), land (12.0%), and dem (10.7%) with a VIF of 2.03 to 9.54 (Table 5, Fig. 4b). The argali models incorporated bio2 (38.1%), popu (37.4%), prec10 (14.2%), and bio14 (10.4%), with VIF values from 1.04 to 5.92 (Table 5 and Fig. 4c). For wild yak, two variables were selected: bio2 (58.2%) and bio17 (41.8%), with VIF values between 1.03 and 3.26 (Table 5 and Fig. 4d).

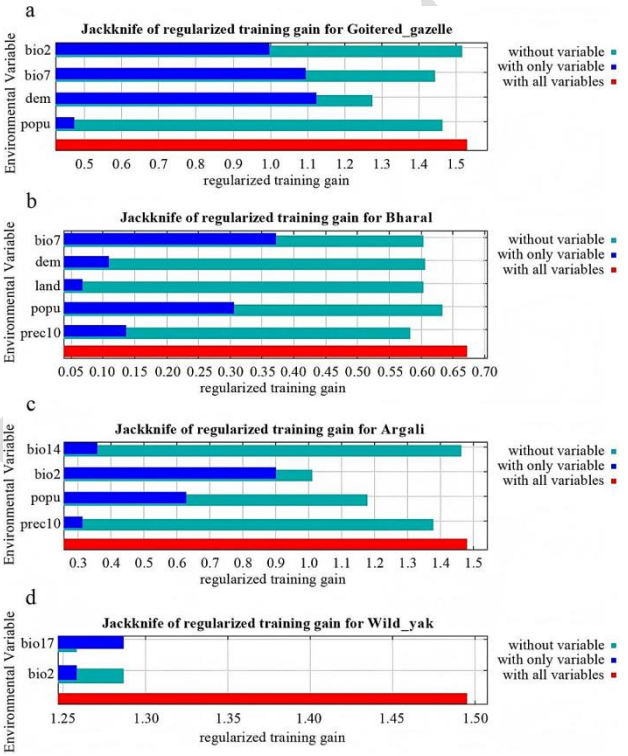

Fig. 4: Outcomes of the Jackknife test to evaluate the significance of variables among four species susceptible to PPRV: (a) goitered gazelle; (b) bharal; (c) argali; and (d) wild yak.

Table 4: PCA of environmental variables for four PPRV-susceptible species

Principal component	Eigenvalues	Percent contribution (%)	Cumulative contribution rate (%)
Goitered Gazelle			
1	53.681	80.122	80.122
2	5.821	8.688	88.809
3	2.544	3.797	92.957
4	1.575	2.351	94.957
5	1.011	1.509	96.456
Bharal			
1	61.098	86.053	86.053
2	4.209	5.929	91.982
3	1.390	1.958	93.940
4	1.114	1.568	95.508
Argali			
1	59.353	88.587	88.587
2	3.778	5.639	94.226
3	1.299	1.939	96.164
Wild yak			
1	57.562	85.913	85.913
2	5.123	7.646	93.559
3	2.416	3.606	97.165

Table 5: Contribution rates of environmental variables of four PPRV-susceptible species

Variables	Percent Contribution (%)	Permutation Importance (%)	VIF
Goitered Gazelle			
dem	50.4	73.9	1.02
bio2	28.6	3	2.35
bio7	10.8	20	3.46
popu	10.2	3.2	6.25
Bharal			
popu	47.9	21.9	2.03
prec10	16.7	18.7	3.56
bio7	12.7	29.2	7.98
land	12.0	5.4	8.23
dem	10.7	24.7	9.54
Argali			
bio2	38.1	60.8	1.04
popu	37.4	30.2	2.95
prec10	14.2	5.9	3.87
bio14	10.4	3.1	5.92
Wild Yak			
bio2	58.2	71.3	1.03
bio17	41.8	28.7	3.26

Model evaluation: Model prediction accuracy was evaluated using ROC curves generated from the MaxEnt model output. The AUC values were 0.950 for goitered gazelle (Fig. 5a), 0.861 for bharal (Fig. 5b), 0.950 for argali (Fig. 5c), 0.924 for wild yak (Fig.5d). The strong predictive performance observed across all species reflects the effectiveness of the variable selection and modeling procedures applied. The combination of dimensionality reduction, multicollinearity control, and spatial filtering contributed to stable model outcomes, as indicated by consistently high AUC values and low variance among bootstrap runs.

Response curves of environmental variables: The distribution of goitered gazelles was influenced by bio2 (mean monthly diurnal temperature range), bio7 (annual temperature range), elevation (dem), and population density (popu). As shown in Fig. 6a, occurrence probability declined as bio2 increased from about 12 to 12.8°C and then showed little further change. In Fig. 6b, probability increased with bio7, reaching its highest value at around 41.6°C, before decreasing and leveling off beyond 42°C. Fig. 6c shows that occurrence was highest at an elevation of approximately 2900m, with lower probabilities at higher elevations. In Fig. 6d, probability decreased steadily with increasing popu, suggesting lower suitability in areas with higher human presence.

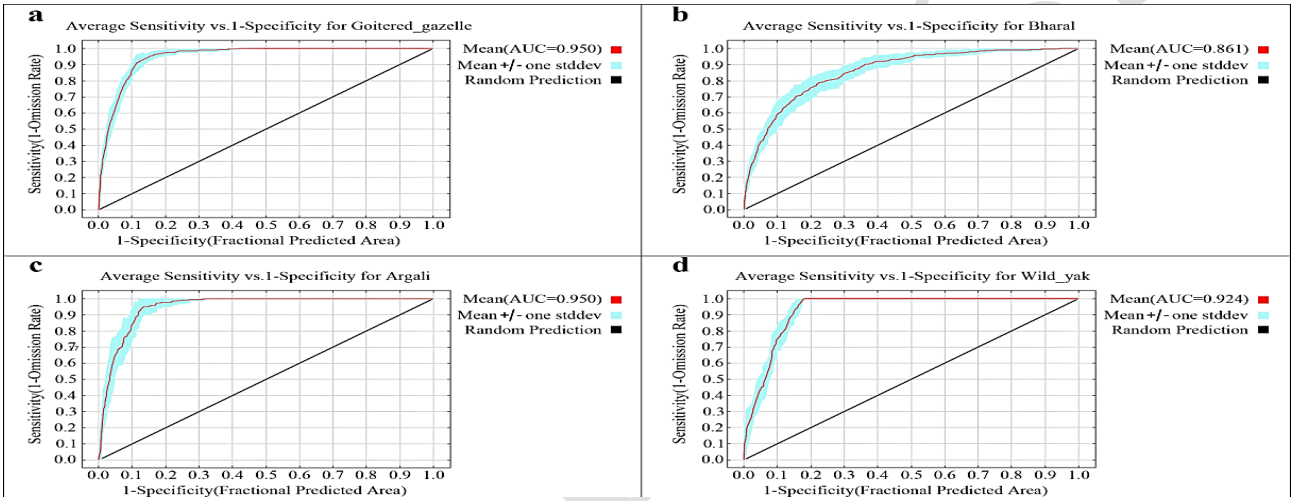

Fig.5: ROC curves were employed to assess the predictive accuracy of MaxEnt distribution models for four wildlife species susceptible to PPRV. The curves and corresponding Area Under the Curve (AUC) values are shown for: (a) Goitered gazelle; (b) Bharal; (c) Argali; and (d) Wild yak. High AUC values, between 0.86 and 0.95, demonstrate outstanding predictive ability in differentiating suitable habitats from unsuitable ones.

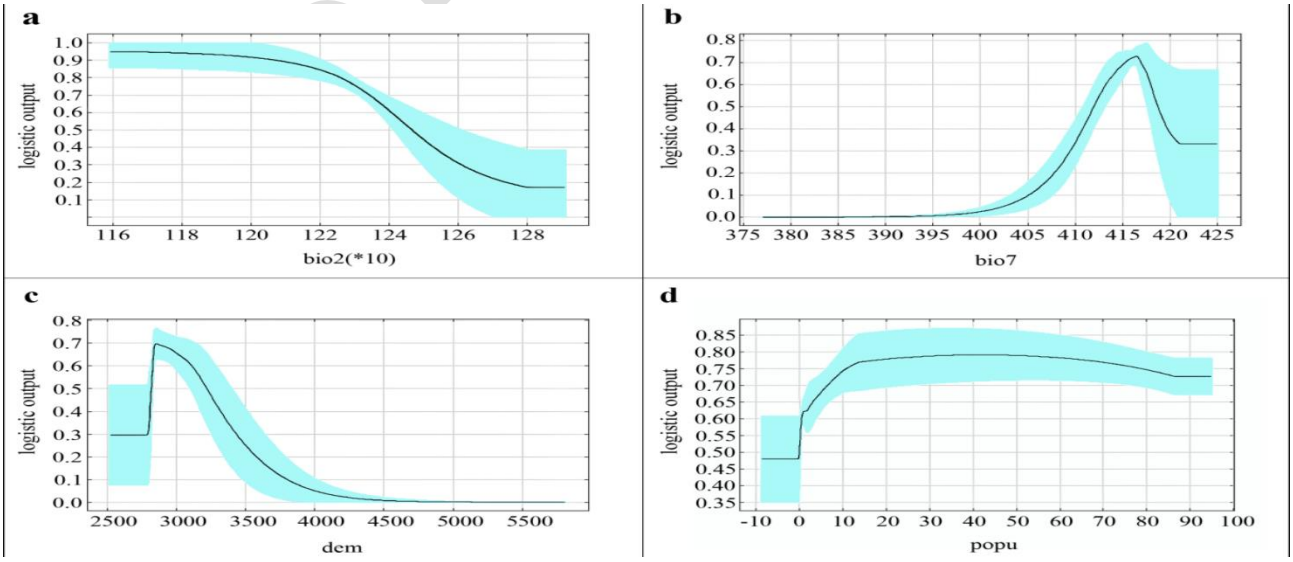

Fig. 6: Charts depicting the impact of crucial environmental variables on the probability of goitered gazelle distribution. (a) mean monthly diurnal range (bio2); (b) annual temperature range (bio7); (c) elevation (dem); and (d) population density (popu). According to the MaxEnt model, each curve shows the relationship between an environmental predictor and the estimated probability of presence.

The distribution of bharal was mainly associated with bio7, elevation (dem), land-cover type (land), population density (popu), and October precipitation (prec10). The distribution probability between 38 and 42°C followed a non-linear pattern, increasing rapidly from 38 to 38.5°C, rising more gradually up to about 40.5°C and then declining sharply toward 42°C (Fig 7a). Elevational responses were variable between 2500 and 4400m (Fig. 7b), after which probability increased markedly, reaching a clear maximum near 5500m. Land cover responses (Fig. 7c) indicated a stronger association with cropland compared with other habitat types. As illustrated in Fig. 7d, probability increased with population density up to a value of approximately 5, beyond, which it declined. In Fig. 7e, probability rose with October precipitation from 0 to 6mm, decreased gradually between 6 and 9mm, and showed little change thereafter.

For argali, distribution patterns were mainly associated with precipitation in the driest month (bio14), bio2, popu, and prec10. As shown in Fig. 8a, probability increased rapidly as bio14 rose from 0 to 0.5mm, followed by a decline up to 5.5 mm. Fig. 8b shows probability increasing with bio2 between 11.8°C and 12°C, then decreasing to a minimum at 12.8°C. Fig. 8c suggests higher probability in areas with lower population density. Fig. 8d indicates increasing probability with prec10 from 0 to 4 mm, beyond which it decreases, reaching a minimum at 9 mm.

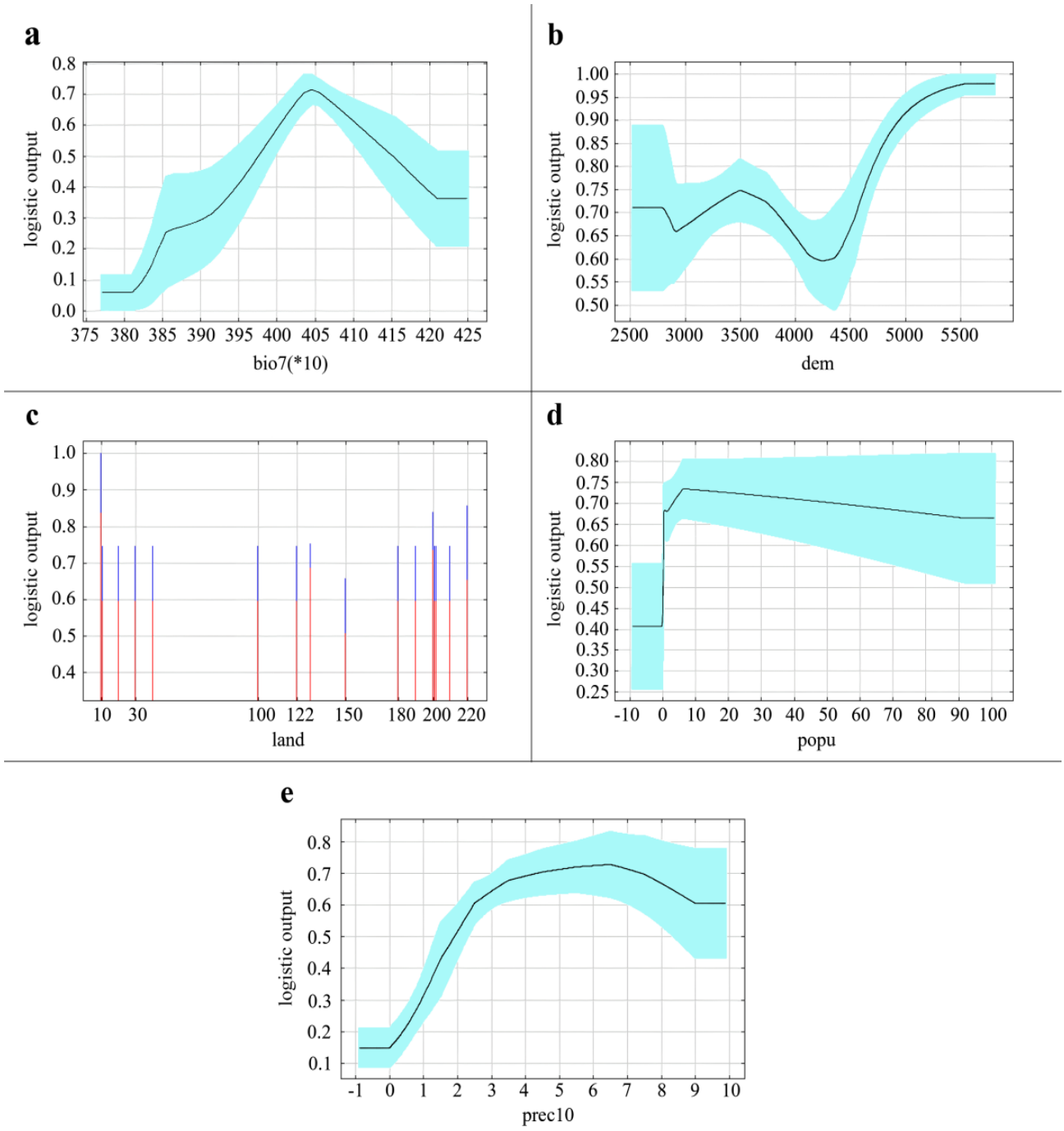

Fig.7: Response curves of key environmental variables influence the distribution probability of bharal. (a) annual temperature range (bio7); (b) elevation (dem); (c) land use (land); (d) population density (popu); and (e) October precipitation (prec10). Each curve represents the link between the environmental predictor and the probability of bharal occurrence according to MaxEnt model predicted.

The distribution of wild yaks was predominantly influenced by bio17 (precipitation in the driest quarter) and bio2. As shown in Fig.9a, probability increased with bio17 from 0 to 18 mm. Fig. 9b indicates the highest probability occurred when bio2 was between 11.6 and 11.7, beyond which it decreased with increasing temperature.

Distribution prediction of PPRV-susceptible wildlife in Huaitoutala Town: The highest distribution probability of goitered gazelle in the Huatoutala region occurred in the southeast, near Kuluk Lake, with suitability gradually decreasing toward the periphery. Overall suitable area was concentrated in the south, while the northern part showed the lowest probability (Fig. 10a). For bharal, the highest distribution probability located in the north-central area, increasing from west to east. In general, probability was higher in northern areas than in southern ones, showing a gradient of increasing suitability from south to north (Fig. 10b). Argali showed the highest distribution probability in the eastern part of Huatoutala, increasing from west to east. Eastern areas exhibited higher suitability compared to the west (Fig. 10c). The probability of distribution of the wild yak is highest in the northeastern region, with suitability increasing from south to north, and the suitability in the northern region is generally higher than that in the southern region (Fig. 10d).

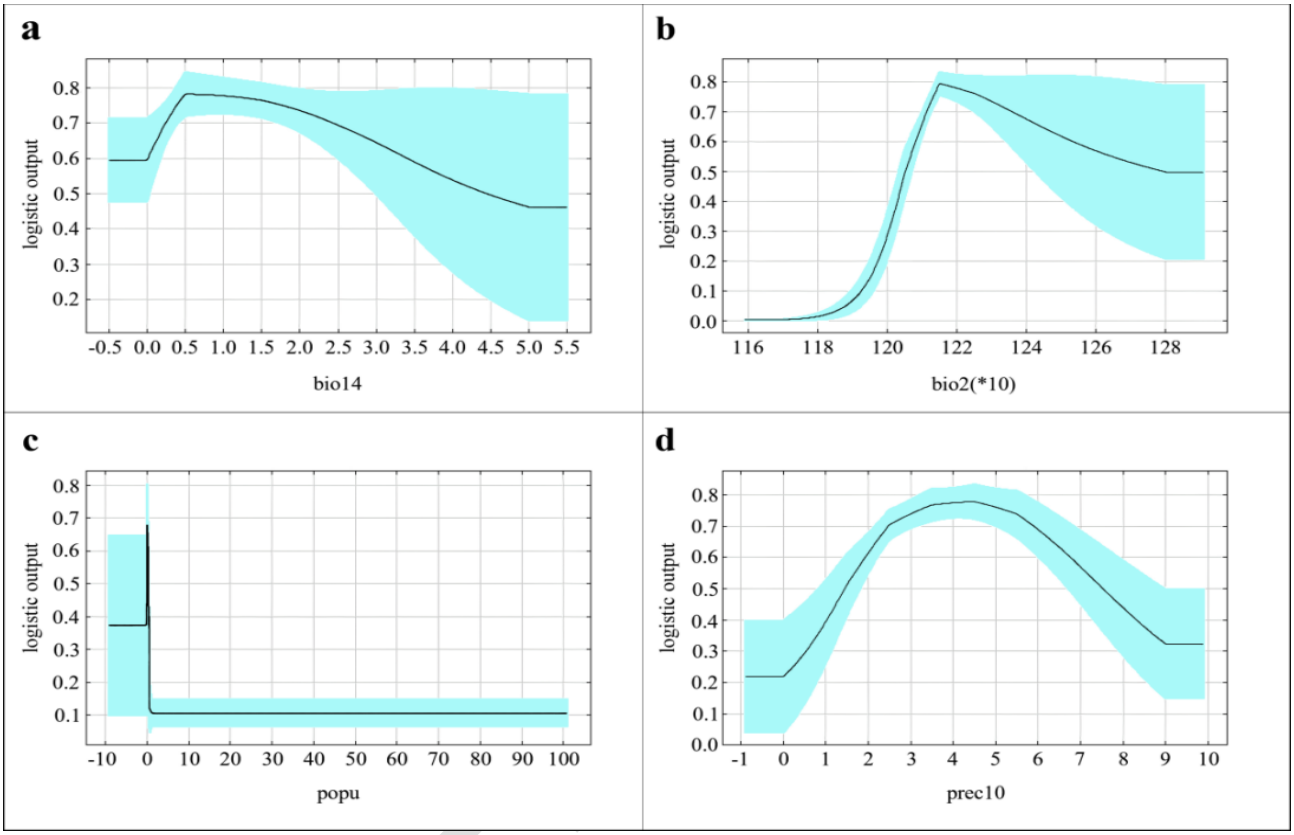

Fig.8: The probability of argali distribution is affected by response curves of significant environmental variables. (a) precipitation of the driest month (bio14); (b) mean monthly diurnal range (bio2); (c) popu; and (d) prec10. The MaxEnt model predicts the probability of argali occurrence, and each curve depicts its relationship with the environmental variable.

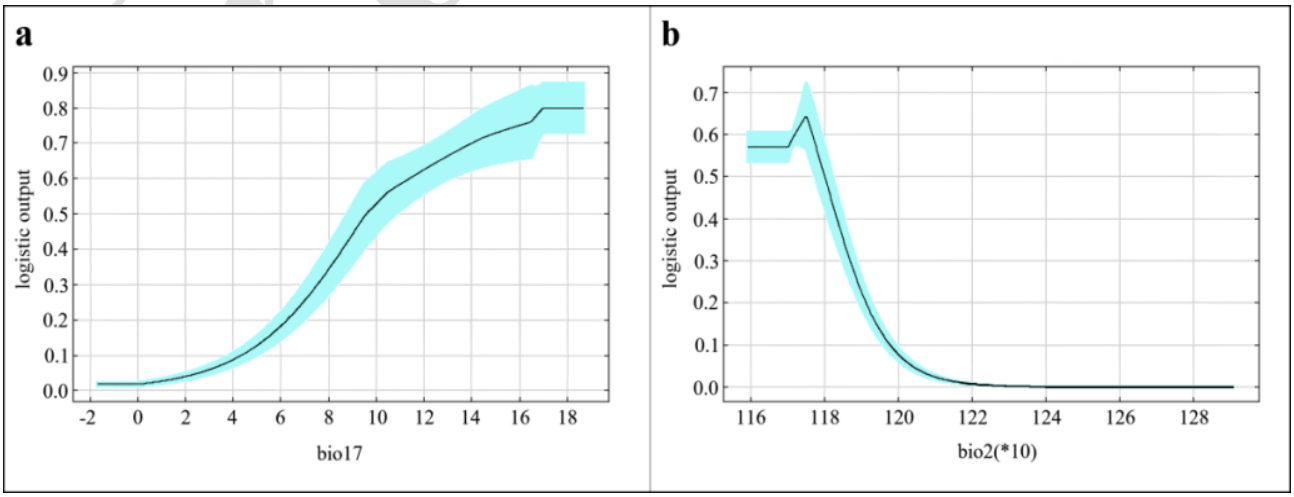

Fig. 9: Response curves of key environmental variables affecting the distribution probability of wild yak. (a) precipitation of the driest quarter (bio17) and (b) bio2. Each curve represents the relationship between a specific variable and the modeled probability of wild yak occurrence in the study area.

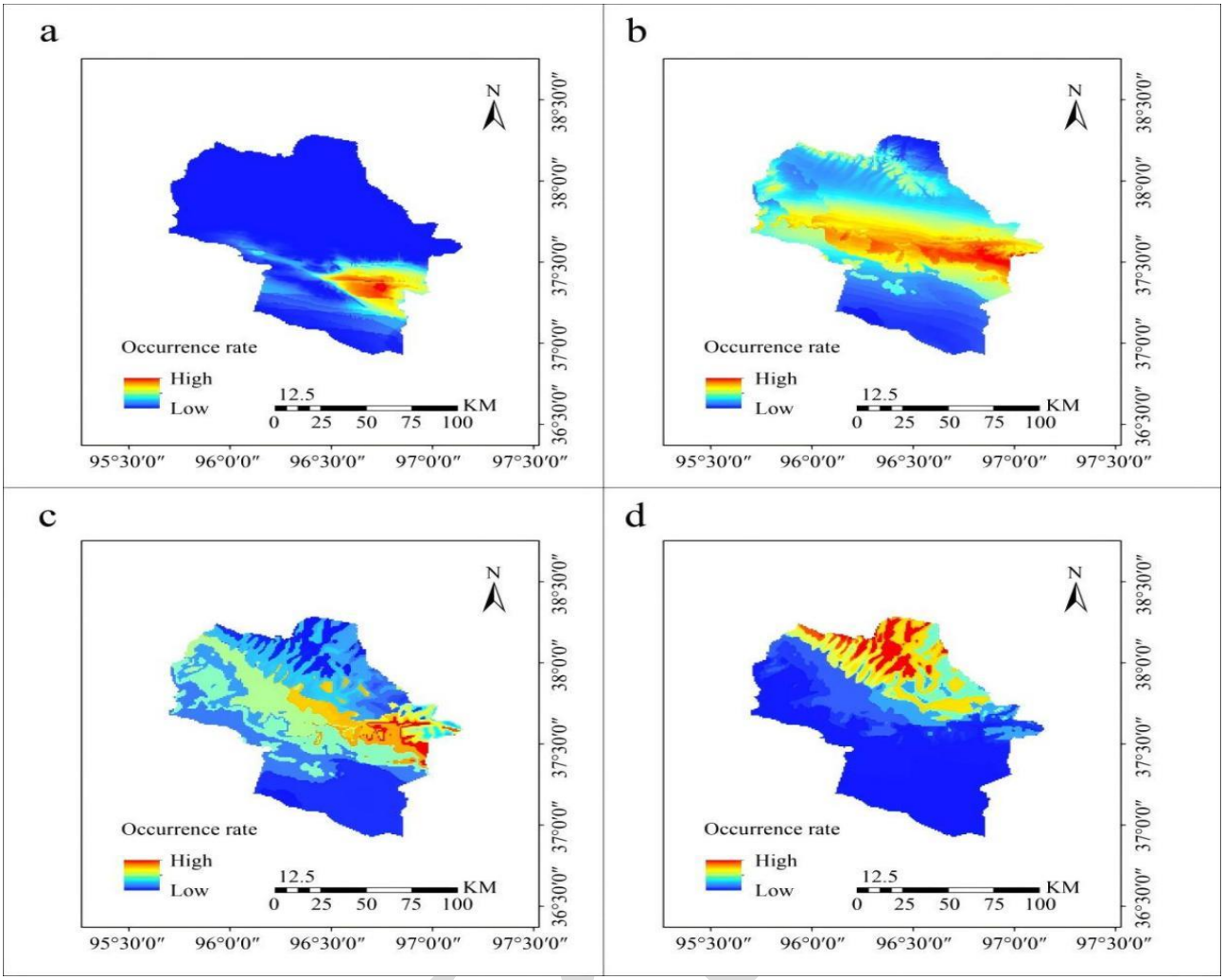

Fig. 10: Predicted habitat suitability maps for four PPRV-susceptible ungulate species in Huaitoutala, Qinghai Province, showing spatial variation from high to low suitability. (a) Goitered gazelle; (b) Bharal; (c) Argali; and (d) Wild yak. The maps were generated using MaxEnt based on environmental and anthropogenic variables.

DISCUSSION

This study focuses on the high-altitude ecosystem of Huaitoutala in Qinghai Province, China, and investigates PPR infection dynamics using combination of ecological modeling and field-based population surveys. The work was conducted in an ecologically fragile area that has received relatively little prior study, with particular attention given to the role of wildlife in PPRV transmission rather than an exclusive focus on livestock. The main objective was to evaluate potential risks at the wildlife-livestock interface and to support the development of predictive approaches for PPR management in sensitive ecosystems.

Population densities of PPRV-susceptible wildlife were derived from line transect surveys analyzed with the Distance software. Estimated densities were 0.329 individuals/km^2 for goral, 0.302 individuals/km^2 for bharal, 0.193 individuals/km^{2}for alpaca, and 0.100 individuals/km^{2}for wild yak. The observed differences in density appear to be associated with species-specific habitat preferences and local environmental conditions, which were also evident in the variation among detection functions related to behavior and habitat use.

The population density estimated for goitered gazelles in Huaitoutala was lower than the value reported from the Junggar Basin in Xinjiang, where 2.013 individuals per km^{2}were recorded in 2002 (Yang *et al*., 2005). The two regions differ in their environmental setting. Huaitoutala is situated along the margin of the Qaidam Basin and is characterized by high elevation and sparse vegetation. In contrast, the Junggar Basin includes more heterogeneous habitats and comparatively higher vegetation productivity.

Bharal were observed at higher densities than argali in the study area. The species is commonly associated with rocky mountain terrain at elevations of approximately 3000–4000 m. In such environments, group formation and cryptic coloration are frequently noted features (Namgail *et al*., 2004). These characteristics are consistent with the broader detection range recorded for bharal during the surveys.

Wild yak showed the lowest estimated population density among the species surveyed. Records for this species were largely confined to alpine meadows and sparsely vegetated mountain areas between 3500 and 4500m. These habitats are characterized by low temperatures, limited forage, and rugged terrain. Genetic studies have reported historical population bottlenecks in wild yak populations (Ma *et al*., 2010). The detection curve for this species was relatively flat, and encounter rates during surveys were low, particularly at greater distances.

Habitat suitability and environmental factors for these wildlife species were evaluated using the MaxEnt model. Model performance was consistently high across species, with all AUC values exceeding 0.85 (Fig. 5a–5d). The highest predictive accuracy was obtained for the goitered gazelle and argali (both AUC = 0.95), followed by wild yak (AUC = 0.92) and bharal (AUC = 0.86). Elevation (50.4%) and bio2 (28.6%) were the most influential variables for goitered gazelle distribution (Fig. 4a), consistent with earlier studies on Tibetan ungulates (Shi *et al*., 2023). Human population density strongly affected bharal (47.9%) (Fig. 4b) and argali (37.4%) (Fig. 4c), exceeding values reported by McDonald *et al*. (2018), reflecting intensified livestock activity in the region. The distribution of wild yak appears closely tied to seasonal precipitation, with bio17 contributing 41.8% of the explanatory power (Fig. 4d). Similar associations were noted by Barroso *et al*. (2024)

The response curves showed different patterns among species. For goitered gazelles, occurrence declined with increasing human population density (Fig. 6d). Bharal showed a non-linear response to human disturbance, with changes occurring around a threshold level (Fig. 7d). Argali records were concentrated in areas with relatively low human density (Fig. 8c). Wild yak occurrence increased with precipitation during the driest quarter (Fig. 9a).

Key environmental variables differ across regions, reflecting underlying climatic and geographic variation. In Qinghai, pronounced day–night temperature changes are a common feature, and temperature-related variables therefore show a stronger signal. In other areas, this pattern is not necessarily observed, and different environmental factors may be more influential. For this reason, epidemiological models of wildlife disease are better interpreted when they are developed in relation to local environmental conditions.

The habitat suitability maps are shown in Fig.10a–10d. Spatial patterns differed among species. Areas of higher suitability for goitered gazelle were mainly located along the southeastern edge of the study area, with a concentration near Kelu Lake; In contrast, suitability for bharal and wild yak was greater in the northern part of the region. Zones where these areas overlap were limited but identifiable, suggesting monitoring and management efforts could be prioritized.

Evidence from other high-altitude systems provides useful references. In the Indian Trans-Himalaya, bharal and argali have both been reported as hosts of PPRV, with bharal typically recorded at higher densities and showing a wider range of habitat use (Namgail *et al*., 2004). A separate case was documented during the 2017–2018 PPR outbreak in Mongolia's Gobi region, where high mortality occurred in Mongolian saiga populations inhabiting arid, high-elevation landscapes (Benfield *et al*., 2021). Studies conducted across the Qinghai–Tibet Plateau have also noted associations between ungulate distribution patterns and factors such as human disturbance and temperature variability (Shi *et al*., 2023).

It is important to note that this study did not involve virological or serological testing. Therefore, the identification of high-suitability areas for PPRV-susceptible wildlife reflects ecological vulnerability rather than confirmed infection. The predicted hotspots represent areas where conditions may facilitate wildlife-livestock interface and potential spillover, rather than locations of active viral transmission. Further validation through field-based virological surveillance is essential to confirm whether these zones correspond to actual infection risk.

As we enlist limitations in this study, the terrain of the study area is highly complex, which created difficulties in survey design and field data collection, and this may have affected measurement accuracy in certain situations. The MaxEnt model showed generally good performance, but uncertainty cannot be fully avoided. This is partly related to spatial inconsistencies in the occurrence data, as well as to the fact that some environmental variables were not available and therefore could not be included in the analysis.

Conclusions: This study adds information on PPRV risk in wild ungulates from Huaitoutala, Qinghai. Wildlife appears to be involved in local transmission processes. Areas where wildlife and livestock occur in close proximity were identified in the analysis, especially where suitable habitat for host species is present. Including wildlife-related data in PPR management may help clarify patterns of disease risk. Maintaining natural habitats could also influence spillover processes and has implications for biodiversity conservation. This study highlights potential ecological risk areas for PPRV spillover based on species distribution and environmental factors. While these results can inform surveillance planning but should not be interpreted as evidence of current viral circulation. Targeted serological and virological investigations are needed to confirm the presence or absence of PPRV in these identified regions.

Conflicts of Interest: The authors have no conflicts of interest to declare.

Funding: No funding.

Author contributions: HNW and XF were responsible for data curation and writing-original draft preparation. GYN was responsible for conceptualization; FYC and RNW were responsible for Methodology; SPY and XDW were responsible for supervision; SFS and XDW were responsible for writing-review and editing. XLW was responsible for writing-review and editing; All authors have read and agreed to the published version of the manuscript.

REFERENCES

Aziz Ul R, Abubakar M, Rasool MH, *et al*., 2016. Evaluation of risk factors for Peste des Petits Ruminants virus in Sheep and Goats at the wildlife-livestock interface in Punjab Province, Pakistan. BioMed Research International 2016:7826245.

Baazizi R, Mahapatra M, Clarke BD, *et al*., 2017. Peste des petits ruminants (PPR): A neglected tropical disease in Maghreb region of North Africa and its threat to Europe. PloS One 12:e0175461.

Brown JL, Bennett JR, French CM, 2017. SDMtoolbox 2.0: the next generation Python-based GIS toolkit for landscape genetic, biogeographic and species distribution model analyses. PeerJ 5:e4095.

Bouchemla F, Sherasiya A, Benseghir H, *et al*., 2020. World epidemiological meta-analyses of peste des petits ruminants (1997-2017). Reviews in Science and Technology 39:871-81.

Benfield CTO, Hill S, Shatar M, *et al*., 2021. Molecular epidemiology of peste des petits ruminants virus emergence in critically endangered Mongolian saiga antelope and other wild ungulates. Virus Evolution 7:veab062.

Barroso P, López-Olvera JR, Kiluba wa Kiluba T, *et al*., 2024. Overcoming the limitations of wildlife disease monitoring. Research Directory: One Health. 2:e3.

Duque-Lazo J, van Gils H, Groen TA, *et al*., 2016. Transferability of species distribution models: The case of *Phytophthora cinnamomi* in Southwest Spain and Southwest Australia. Ecological Modelling 320:62-70.

Duque-Lazo J, Navarro-Cerrillo RM, van Gils H, *et al*., 2018. Forecasting oak decline caused by *Phytophthora cinnamomi* in Andalusia: Identification of priority areas for intervention. Forest Ecology and Management 417:122-36.

Dou Y, Liang Z, Prajapati M, *et al*., 2020. Expanding diversity of susceptible hosts in Peste Des Petits Ruminants virus infection and its potential mechanism beyond. Frontiers in Veterinary Science 7:66.

Fekede RJ, van Gils H, Huang L, *et al*., 2019. High probability areas for ASF infection in China along the Russian and Korean borders. Transboundary Emerging Diseases 66:852-64.

Gao S, Xu G, Zeng Z, *et al*., 2021. Transboundary spread of peste des petits ruminants virus in western China: A prediction model. PloS One 16:e0257898.

Harris RB, 2010. Rangeland degradation on the Qinghai-Tibetan plateau: A review of the evidence of its magnitude and causes. Journal of Arid Environment 74:1-12.

Harman RR, Kim TN, 2024. Differentiating spillover: an examination of cross-habitat movement in ecology. Proceedings of the Royal Society B: Biological Sciences 291:20232707.

Jones BA, Rich KM, Mariner JC, *et al*., 2016. The economic impact of eradicating Peste des Petits Ruminants: A benefit-cost analysis. PloS One 11:e0149982.

Lembo T, Oura C, Parida S, *et al*., 2013. Peste des petits ruminants infection among cattle and wildlife in northern Tanzania. Emerging Infectious Diseases 19:2037.

Liu F, Li J, Li L, *et al*., 2018. Peste des petits ruminants in China since its first outbreak in 2007: A 10-year review. Transboundary and Emerging Diseases 65:638-648.

Ma Z, Zhong J, Han J, *et al*., 2010. Genetic diversity and demographic history of wild Yak (*Bos grunniens* mutus) inferred from mtDNA D-loop sequences[J]. African Journal of Biotechnology 9(46):7805-7810

Munir M, 2014. Role of wild small ruminants in the epidemiology of peste des petits ruminants. Transboundary and Emerging Diseases 61:411-24.

Moriguchi S, Onuma M, Goka K, 2016. Spatial assessment of the potential risk of avian influenza A virus infection in three raptor species in Japan. Journal of Veterinary Medical Science 78:1107-15.

McDonald JL, Robertson A, Silk MJ, 2018. Wildlife disease ecology from the individual to the population: Insights from a long-term study of a naturally infected European badger population. Journal of Animal Ecology 87:101-12.

Namgail T, Fox JL, Bhatnagar YV, 2004. Habitat segregation between sympatric Tibetan argali Ovis ammon hodgsoni and blue sheep Pseudois nayaur in the Indian Trans-Himalaya. Journal of Zoology 262:57-63.

Pepe M, Longton G, Janes H, 2009. Estimation and comparison of receiver operating characteristic curves. The Stata Journal 9:1.

Pittiglio C, Skidmore AK, van Gils HAMJ, *et al*., 2012. Identifying transit corridors for elephant using a long time-series. International Journal of Applied Earth Observation and Geoinformation 14:61-72.

Sowjanya SK, Bhavya AP, Akshata N, *et al*., 2021. Peste Des Petits Ruminants in atypical hosts and wildlife: Systematic review and meta-analysis of the prevalence between 2001 and 2021. Archives of Razi Institute 76:1589-606.

Shi F, Liu S, An Y, *et al*., 2023. Climatic factors and human disturbance influence ungulate species distribution on the Qinghai-Tibet Plateau. Science of the Total Environment 869:161681.

Thomas L, Buckland ST, Rexstad EA, *et al*., 2010. Distance software: design and analysis of distance sampling surveys for estimating population size. Journal of Applied Ecology 47:5-14.

Van Gils H, Westinga E, Carafa M, *et al*., 2014. Where the bears roam in Majella National Park, Italy. Journal of Nature Conservation 22:23-34.

Wensman JJ, Abubakar M, *et al*., 2018. Peste des petits ruminants in wild ungulates. Tropical Animal Health and Production 50:1815-9.

Yang W, Qiao J, Yao J, *et al*., 2005. Characteristics of foraging habitat of Goitred Gazelles (*Gazella subgutturosa* sairensis) in Eastern Junggar Basin, Xinjiang. Acta Theriologica Sinica 25:355-60.

Zahur AB, Ullah A, Hussain M, *et al*., 2011. Sero-epidemiology of peste des petits ruminants (PPR) in Pakistan. Preventive Veterinary Medicine 102:87-92.